

A concentric planar doubly π -aromatic B_{19}^- cluster

Wei Huang¹, Alina P. Sergeeva², Hua-Jin Zhai¹, Boris B. Averkiev², Lai-Sheng Wang^{1*} and Alexander I. Boldyrev^{2*}

Atomic clusters often show unique, size-dependent properties and have become a fertile ground for the discovery of novel molecular structures and chemical bonding. Here we report an investigation of the B_{19}^- cluster, which shows chemical bonding reminiscent of that in [10]annulene ($C_{10}H_{10}$) and [6]circulene ($C_{24}H_{12}$). Photoelectron spectroscopy reveals a relatively simple spectrum for B_{19}^- , with a high electron-binding energy. Theoretical calculations show that the global minimum of B_{19}^- is a nearly circular planar structure with a central B_6 pentagonal unit bonded to an outer B_{13} ring. Chemical bonding analyses reveal that the B_{19}^- cluster possesses a unique double π -aromaticity in two concentric π -systems, with two π -electrons delocalized over the central pentagonal B_6 unit and another ten π -electrons responsible for the π -bonding between the central pentagonal unit and the outer ring. Such peculiar chemical bonding does not exist in organic compounds; it can only be found in atomic clusters.

Aromaticity in chemistry manifests itself as enhanced stability, high symmetry, low reactivity, bond-length equalization, enhanced anisotropy of diamagnetic susceptibility, diatropic (low-field) 1H NMR shifts, large negative nucleus-independent chemical shift (NICS) values and high-electron detachment energies in photoelectron spectra^{1–3}. Aromaticity in conjugated hydrocarbons follows Hückel's ($4n+2$) π -electron rule, which was developed on the basis of the symmetry of molecular orbitals of monocyclic C_nH_n (where n is an even number) hydrocarbons, known in chemistry as annulenes. The prototypical aromatic molecule with six π -electrons that satisfies the $4n+2$ rule is benzene or [6]annulene ($n=1$). The next uncharged homologue of benzene with $n=2$ is [10]annulene ($C_{10}H_{10}$, planar monocyclic cyclodeca-1,3,5,7,9-pentaene) (Fig. 1a,i). However, [10]annulene was shown to be neither planar nor aromatic^{4–6}. Masamune and co-workers isolated two crystalline forms (A and B) of [10]annulene and came to the conclusion that both possessed non-planar geometries^{4,5}.

The most recent *ab initio* calculations⁶ showed the three isomers of lowest energy for $C_{10}H_{10}$, all as non-planar species: a 'twist' structure (the most stable), and a 'naphthalene-like' structure and a 'heart-shaped' structure (each with 1.4 kcal mol⁻¹ and 4.2 kcal mol⁻¹, respectively, more energy than the twist structure), all calculated at a high level of theory. Price and Stanton demonstrated that the 'twist' isomer corresponds to the crystalline form B of $C_{10}H_{10}$ by comparing experimental NMR shifts with theoretical calculations⁷. The planar monocyclic [10]annulene (Fig. 1a) is substantially higher in energy and not even a local minimum on the potential energy surface. The concept of aromaticity has long been extended to realms outside those of organic chemistry^{2,3,8}. The question is whether we can find analogous ten π -electron systems among other classes of chemical species. Boron clusters could potentially offer such an opportunity, as a number of hydrocarbon analogues of boron clusters have been identified recently^{9–16}.

Chemical bonding, structure, reactivity and stability of planar and quasi-planar boron clusters can be rationalized using concepts of aromaticity and antiaromaticity^{9–16}. In particular, B_8^{2-} and B_9^- (refs 9,16), B_{10} , B_{11}^- and B_{12} (ref. 10), and B_{13}^+ boron clusters^{11–15} can be viewed as all-boron analogues of benzene on the basis of their six π -electrons, as they have π -molecular orbital patterns

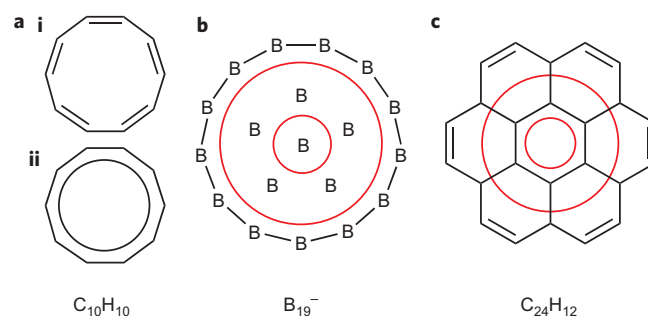


Figure 1 | Comparison of the structure and chemical bonding of B_{19}^- with two hydrocarbon molecules. a–c, All the schemes show localized 2c–2e σ - and π -bonds (C–C σ -bonds, B–B σ -bonds and C–C π -bonds represented as single lines, with the C–H σ -bonds omitted) and delocalized π -bonds (represented as circles). a, [10]annulene ($C_{10}H_{10}$) exists in the non-planar form (i) and features localized bonding only (classic molecule, non-aromatic); ii, the model planar [10]annulene ($C_{10}H_{10}$) has a circular structure with ten π -electrons delocalized over the peripheral ring of carbon atoms ($4n+2=10$, $n=2$, π -aromatic). b, B_{19}^- consists of two concentric π -systems with two π -electrons delocalized over the central pentagonal B_6 unit ($4n+2=2$, $n=0$, π -aromatic) and ten additional π -electrons delocalized in a circle between the central B_6 unit and the outer B_{13} ring ($4n+2=10$, $n=2$, π -aromatic), as well as 13 peripheral B–B σ -bonds. The six central boron atoms do not participate in the localized σ -bonding, but rather in delocalized σ -bonding. c, [6]circulene, or coronene ($C_{24}H_{12}$), is composed of six benzene rings with π -bonding that consists of three parts: (1) six localized 2c–2e C–C peripheral π -bonds, (2) six π -electrons delocalized over the central C_6 ring ($4n+2=6$, $n=1$, π -aromatic) and (3) six delocalized π -electrons responsible for the bonding between the inner C_6 ring and the outer C_{18} ring ($4n+2=6$, $n=1$, π -aromatic).

similar to those of benzene. Early experimental work on boron clusters involved measurements of appearance potentials and fragmentation patterns using collision-induced dissociations^{17–21}, which revealed that B_{13}^+ has anomalously high stability and low reactivity in comparison with other cationic boron clusters, consistent with its aromatic nature. Recently, photoelectron spectroscopy

¹Department of Chemistry, Brown University, Providence, Rhode Island 02912, USA, ²Department of Chemistry and Biochemistry, Utah State University, Logan, Utah 84322-0300, USA. *e-mail: a.i.boldyrev@usu.edu; lai-sheng_wang@brown.edu

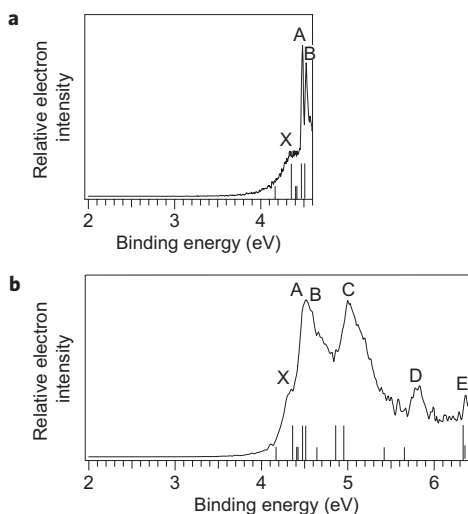


Figure 2 | Photoelectron spectra of B_{19}^- . **a,b**, Shown are spectra at 266 nm (4.661 eV) (**a**) and at 193 nm (6.424 eV) (**b**). The calculated vertical electron-detachment energies for two isomers of B_{19}^- are represented as the vertical bars. The long bars correspond to the VDEs calculated for the global minimum isomer I and the short bars for the low-lying isomer II.

in combination with *ab initio* calculations enabled detailed structural characterization of a series of boron clusters^{9–11,22–25}, and led to the concept of hydrocarbon analogues of planar boron clusters. The latest example is B_{16}^{2-} with ten π -electrons, which was shown to be an all-boron analogue of naphthalene²⁶.

Here we report an experimental and theoretical investigation of the B_{19}^- cluster. We found that B_{19}^- possesses a nearly circular planar structure (Fig. 1b) with a pentagonal central B_6 unit within a B_{13} ring and a π -bonding pattern that displays similarities to those of both the planar aromatic [10]annulene (Fig. 1a,i) and [6]circulene (Fig. 1c). The representation of the structure and chemical bonding of [6]circulene given here avoids resonance description and is consistent with the symmetry of the molecule (Fig. 1c). It was first proposed by Zubarev and Boldyrev²⁷ and is not as well-known among organic chemists as the resonance structures widely used in the literature (see Fig. S1). According to the Zubarev and Boldyrev representation, in [6]circulene 96 valence electrons of the total 108 participate in the localized bonding: 60 comprise 30 $2c-2e$ C–C σ -bonds, 24 comprise 12 $2c-2e$ C–H σ -bonds and 12 comprise six $2c-2e$ C–C π -bonds. The other 12 valence electrons participate in delocalized π -bonding. The $4n + 2$ rule is applied to the two π -subsystems separately: six π -electrons

are responsible for the bonding in the internal six carbon atoms ($4n + 2 = 6$, $n = 1$), and the other six π -electrons are responsible for the bonding between the peripheral C_{18} and the internal C_6 rings ($4n + 2 = 6$, $n = 1$). π -bonding in B_{19}^- consists of two concentric π -systems, analogous to [6]circulene, with two π -electrons delocalized over the central pentagonal unit and ten additional π -electrons delocalized in a circle between the central B_6 unit and the outer B_{13} ring, reminiscent of the ten π -electrons in the planar [10]annulene (Fig. 1b).

The experiment was carried out using a magnetic bottle photoelectron spectroscopy apparatus equipped with a laser vaporization source (see Methods)²⁸. Photoelectron spectra of B_{19}^- at two photon energies are shown in Fig. 2, in which they are compared with the calculated vertical detachment energies (VDEs). The 193 nm spectrum (Fig. 2b) shows five resolved bands. At 266 nm (Fig. 2a) the band at 4.5 eV resolved into two sharp peaks (A and B). The ground state band (X) was observed to be fairly broad in the 266 nm spectrum, which suggests a possible geometry change between the anion and neutral ground state. The adiabatic detachment energy of B_{19}^- was estimated as 4.2 ± 0.1 eV, which is very high. The VDEs of all the spectral features are given in Table 1 and compared to the theoretical VDEs (see Methods) of the two isomers of B_{19}^- with the lowest energies (isomers I and II).

We searched for the global minimum of B_{19}^- using two programs: a Coalescence Kick²⁹ program written by B. B. Averkiev and a basin hopping search³⁰ program written by W. Huang, both initially at the B3LYP/3-21G level of theory. The Coalescence Kick method subjects large populations of randomly generated structures to a coalescence procedure in which all atoms are pushed gradually to the molecular centre of mass to avoid the generation of fragmented structures and then optimizes them to the nearest local minima. Basin hopping is an unbiased global minimum search method, in which potential energy transformation is combined with Monte Carlo sampling. All low-lying isomers found by both methods were reoptimized at the B3LYP/6-311 + G^* level of theory, with further single-point calculations at the CCSD(T)/6-311 + G^* level of theory using the optimized geometry at the B3LYP/6-311 + G^* level. The three structures of lowest energy, together with a tubular structure, are summarized in Fig. 3. A more extensive set of alternative structures is given in the Supplementary Information (Fig. S2).

We found that the global minimum of B_{19}^- (Fig. 3a) is a planar ‘spider-web’ structure with one boron atom at the centre surrounded by five boron atoms in the first coordination sphere and 13 boron atoms in the second coordination sphere. The geometric parameters presented in Fig. S3 suggest an almost perfect planar and circular structure for the global minimum of B_{19}^- . The distances from the

Table 1 | Comparison of experimental VDEs (VDE_{exp}) and calculated VDEs (VDE_{theo}) for isomers I and II of B_{19}^- (eV).

Feature	VDE_{exp}	Final state and electronic configuration	VDE_{theo} (TD-B3LYP)
Isomer I			
X	4.34 ± 0.05	${}^2B_1, \{ \dots 1a_2^{(2)}13a_1^{(2)}10b_2^{(2)}3b_1^{(2)}2a_2^{(2)}4b_1^{(1)} \}$	4.37
A	4.48 ± 0.02	${}^2A_2, \{ \dots 1a_2^{(2)}13a_1^{(2)}10b_2^{(2)}3b_1^{(2)}2a_2^{(1)}4b_1^{(2)} \}$	4.48
B	4.52 ± 0.02	${}^2B_1, \{ \dots 1a_2^{(2)}13a_1^{(2)}10b_2^{(2)}3b_1^{(1)}2a_2^{(2)}4b_1^{(2)} \}$	4.51
C	~ 5.0	${}^2B_2, \{ \dots 1a_2^{(2)}13a_1^{(2)}10b_2^{(1)}3b_1^{(2)}2a_2^{(2)}4b_1^{(2)} \}$	4.88
E	6.37 ± 0.04	${}^2A_1, \{ \dots 1a_2^{(2)}13a_1^{(1)}10b_2^{(2)}3b_1^{(2)}2a_2^{(2)}4b_1^{(2)} \}$ ${}^2A_2, \{ \dots 1a_2^{(1)}13a_1^{(2)}10b_2^{(2)}3b_1^{(2)}2a_2^{(2)}4b_1^{(2)} \}$	4.97 6.34
Isomer II			
Tail	~ 4.1	${}^2B_1, \{ \dots 12a_1^{(2)}9b_2^{(2)}10b_2^{(2)}3b_1^{(2)}2a_2^{(2)}13a_1^{(2)}4b_1^{(1)} \}$ ${}^2A_1, \{ \dots 12a_1^{(2)}9b_2^{(2)}10b_2^{(2)}3b_1^{(2)}2a_2^{(2)}13a_1^{(1)}4b_1^{(2)} \}$ ${}^2A_2, \{ \dots 12a_1^{(2)}9b_2^{(2)}10b_2^{(2)}3b_1^{(2)}2a_2^{(1)}13a_1^{(2)}4b_1^{(2)} \}$ ${}^2B_1, \{ \dots 12a_1^{(2)}9b_2^{(2)}10b_2^{(2)}3b_1^{(1)}2a_2^{(2)}13a_1^{(2)}4b_1^{(2)} \}$	4.19 4.40 4.41 4.64
D	5.8 ± 0.1	${}^2B_2, \{ \dots 12a_1^{(2)}9b_2^{(2)}10b_2^{(1)}3b_1^{(2)}2a_2^{(2)}13a_1^{(2)}4b_1^{(2)} \}$ ${}^2B_2, \{ \dots 12a_1^{(2)}9b_2^{(1)}10b_2^{(2)}3b_1^{(2)}2a_2^{(2)}13a_1^{(2)}4b_1^{(2)} \}$ ${}^2A_1, \{ \dots 12a_1^{(1)}9b_2^{(2)}10b_2^{(2)}3b_1^{(2)}2a_2^{(2)}13a_1^{(2)}4b_1^{(2)} \}$	5.42 5.67 6.36

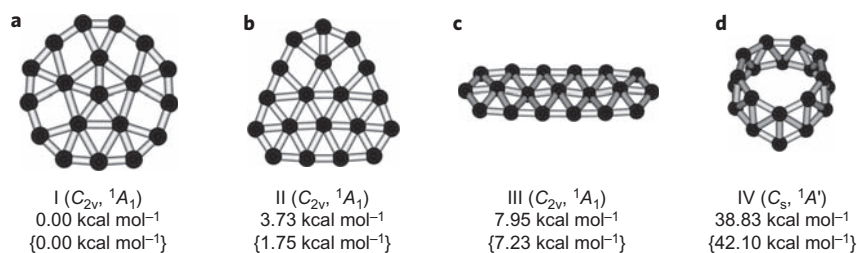


Figure 3 | Four representative optimized isomers of B_{19}^- . **a–d**, The relative energies are given at B3LYP/6-311 + G^* and at CCSD(T)/6-311 + G^* , with the optimized B3LYP/6-311 + G^* geometry given in curly brackets, both corrected for zero-point energies at B3LYP/6-311 + G^* .

central boron atom to the peripheral atoms vary from 3.01 to 3.28 Å, with a maximum deviation from the average distance (3.20 Å) of 0.19 Å or 6%. The appearance of the nearly D_{5h} central B_6 unit (with a maximum of 0.02 Å deviation from the average radius of 1.63 Å) is also quite intriguing as it is reminiscent of bulk boron, which consists of B_{12} icosahedral cages with local C_{5v} symmetry³¹. This structure is of C_s symmetry ($1A'$), but after vibrational averaging it is effectively of C_{2v} symmetry ($1A_1$). The difference in total energies between the C_s and C_{2v} structures is smaller than the difference in zero-point energy corrections for these two structures, with the zero-point energy for the C_s structure being slightly larger. Thus, after zero-point energy correction the C_{2v} effective structure is of lower energy than the C_s structure.

There is only one low-lying isomer (Fig. 3b), which is 1.75 kcal mol⁻¹ higher in energy than the global minimum. The second low-lying isomer (Fig. 3c) was found to be 7.23 kcal mol⁻¹ above the global minimum. The tubular isomer (Fig. 3d), which was the global minimum for the B_{19}^+ cation³², was found to be an isomer of B_{19}^- of very high energy.

The calculated VDEs of the global minimum are in excellent agreement with the experimental data, as shown in Fig. 2 and Table 1. The first VDE was calculated as 4.37 eV compared to the experimental value of 4.34 eV. The next two detachment channels were calculated to be very close in energy, in exact agreement with the A and B bands resolved in the 266 nm spectrum (Fig. 2a). The fourth and fifth detachment channels were also close in energy and corresponded to the C band, which is fairly broad, and contained two unresolved bands (Fig. 2b). The next detachment channel from the global minimum occurred at 6.34 eV, in good agreement with the observed band E at 6.37 eV. The global minimum B_{19}^- had no detachment channel between 5 and 6 eV. Thus, the D band at 5.8 eV cannot emanate from the global

minimum isomer. However, the sixth detachment channel of isomer II, with a calculated VDE of 5.67 eV, is in good agreement with band D, which provides evidence that this isomer was populated in our experiment. The other detachment channels of isomer II can also be discerned from the experimental data, as shown in Fig. 2, although they were not well resolved. In particular, the first detachment channel of isomer II clearly contributed to the lower energy tail of band X. Overall, the agreement between the theoretical and experimental data is excellent, and provides considerable credence to the identified global minimum of B_{19}^- and its low-lying isomer.

Molecular orbital analyses showed that 12 π -electrons in isomer I of B_{19}^- occupied six π -canonical molecular orbitals (CMOs) of two types, as illustrated in Fig. 4. We found five CMOs that contributed to the bonding between the inner pentagonal ring and the outer B_{13} ring, namely HOMO-1, HOMO-2, HOMO-5, HOMO-7 and the sum of HOMO and HOMO-15, which results in a CMO delocalized over the peripheral atoms with no electron density over the pentagonal boron B_6 unit. The remaining π -bond derived from the difference between HOMO and HOMO-15 gives rise to a CMO with electron density across the pentagonal boron B_6 unit and only contributes to the bonding in the inner B_6 unit. The two types of π -bonds can be better interpreted by applying the recently developed adaptive natural density partitioning (AdNDP) analysis³³, as shown in Fig. S4.

The AdNDP analysis is based on the concept of electron pairs as the main elements of chemical bonding. It represents the electronic structure in terms of n -centre two-electron (nc -2e) bonds. The n values range from one to the total number of atoms in the whole cluster, and AdNDP recovers both Lewis bonding elements (1c-2e or 2c-2e objects (that is, lone pairs or conventional two-centre two-electron bonds) and nc -2e delocalized bonding elements,

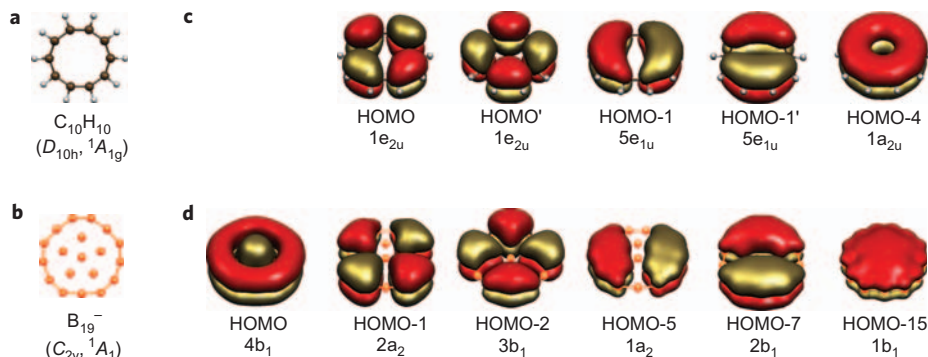


Figure 4 | Comparison of the structures and canonical molecular orbitals between [10]annulene ($C_{10}H_{10}$) and the global minimum of B_{19}^- . **a–d**, The similarity of the π -system of the planar aromatic [10]annulene (**a**) to the ten π -electron subsystem of B_{19}^- (**b**) is illustrated. **c**, The canonical molecular orbitals of [10]annulene ($C_{10}H_{10}$), HOMO, HOMO', HOMO-1, HOMO-1' and HOMO-4. **d**, Five canonical molecular orbitals, HOMO-1, HOMO-2, HOMO-5, HOMO-7 and the sum of HOMO and HOMO-15, of the global minimum of B_{19}^- contribute to the bonding between the inner pentagonal B_6 ring and the outer B_{13} ring, which results in an orbital delocalized over the peripheral atoms with no electron density over the pentagonal B_6 unit, reminiscent of those of [10]annulene (HOMO, HOMO', HOMO-1, HOMO-1' and HOMO-4, respectively) shown in (**c**).

which are associated with the concepts of aromaticity. Both CMO and AdNDP analyses reveal that the chemical bonding in the B_{19}^- cluster consists of two concentric π -aromatic systems: a ten π -electron system that describes the bonding between the inner and outer rings as well as between boron atoms in the peripheral ring and a two π -electron system delocalized over the central B_6 unit, both of which satisfy the $4n + 2$ Hückel rule independently. The ten π -electron subsystem is similar to the π -system in the planar aromatic [10]annulene (Fig. 1a).

The aromaticity of the circular B_{19}^- is also confirmed by NICS analyses³⁴, bond equalization in the outer and inner B_{13} and B_5 rings, and its high VDE of 4.34 eV. In Table S1 we compare the NICS_{zz} values of the circular B_{19}^- with those of benzene and the planar aromatic [10]annulene. The NICS_{zz} value of B_{19}^- is positive close to the plane of the cluster, but becomes negative at 0.4 Å, and attains a maximum negative value of -14.9 parts per million at 0.6 Å above the plane of the cluster. Although the magnitudes of the negative NICS_{zz} values of B_{19}^- are smaller than those for benzene and [10]annulene (Table S1), they clearly show that the circular B_{19}^- cluster is a π -aromatic system.

The concentric aromatic π -systems of the circular B_{19}^- are reminiscent of the π -bonding in circulenes³⁵. Circulenes are cyclic aromatic hydrocarbon compounds and they can be viewed as fused benzene rings; of these [6]circulene (or coronene (Fig. 1c)), which consists of six benzene rings, is a perfect planar D_{6h} molecule. Recent analysis of the chemical bonding of coronene²⁷ showed that its π -bonding consists of three parts: (1) six C-C peripheral π -bonds, (2) three π -bonds delocalized over the central C_6 ring and (3) three delocalized π -bonds responsible for the bonding between the inner C_6 ring and the outer C_{18} ring. The difference between coronene and B_{19}^- is that the former has six π -electrons delocalized over the central part of the molecule and six π -electrons responsible for the bonding between the inner and outer rings, whereas B_{19}^- has only two electrons delocalized over its inner six boron atoms and ten π -electrons responsible for the bonding between the inner and outer rings. Thus, although there is similarity between the π -bonding of the B_{19}^- cluster and coronene, the π -bonding pattern in the boron cluster is unique and does not have an exact counterpart in hydrocarbons.

Interestingly, our structure and bonding analyses showed that the low-lying isomer II of B_{19}^- (Fig. S5) is also doubly π -aromatic with two similar concentric π -systems (Figs S6 and S7), as in isomer I, even though isomer II is much less circular. The key structural difference between the two isomers is the arrangement of the central B_6 unit. In isomer I, the B_6 unit is pentagonal with near D_{5h} symmetry, which results in its nearly circular structure, whereas in isomer II the B_6 unit forms a triangle, which gives rise to the overall triangular shape of this isomer. It is conceivable that the less delocalized π -bonding in isomer II makes it slightly less stable.

In reality, [10]annulene is not a planar species. Our AdNDP analysis for a planar [10]annulene (Fig. S8) revealed ten 2c-2e C-C σ -bonds, ten 2c-2e C-H σ -bonds and five 10c-2e delocalized π -bonds that look exactly the same as the canonical π -molecular orbitals in B_{19}^- , if the π orbital on the inner B_6 unit is ignored (Fig. 4). However, the unfavourable C-C-C bond angles (144° instead of the ideal 120° for sp^2 hybridization) cause substantial strain energies in [10]annulene (Fig. 1a). Apparently, these strain energies outweigh the stabilizing resonance energy derived from π -aromaticity and lead to the out-of-plane distortions in the cyclic $C_{10}H_{10}$ molecule. Thus, boron clusters may provide even more opportunities or flexibility than hydrocarbons for the design of planar aromatic species.

The concentric π -aromatic systems in the global minimum of B_{19}^- can give rise to ring currents either, in the same direction or in the opposite direction to each other, which would be interesting to investigate. The current finding suggests that even more

interesting structures and chemical bonding may be discovered in more complex cluster systems, and so expand established chemical concepts, and they may find applications in nanotechnology. In particular, it may be possible to design doubly aromatic hetero-clusters by replacing the central B_6 unit in the global minimum of B_{19}^- (for example, by transition metals), which may give rise to concentric δ -aromatic and π -aromatic systems. Such modifications may lead to novel boron-based nanosystems with tunable electronic, optical and magnetic properties.

Methods

Experiment. The B_{19}^- cluster was produced by laser vaporization of a ¹⁰B-enriched disc target with a helium carrier and was mass-selected using time-of-flight mass spectrometry. Photoelectron spectra were obtained using a magnetic bottle electron analyser at two photon energies and calibrated by the known spectra of Au^- . The resolution of our photoelectron apparatus was $\Delta E/E \sim 2.5\%$ (that is ~ 25 meV for 1 eV electrons)²⁸.

Theory. The VDEs of B_{19}^- were calculated using the time-dependent hybrid density functional method (TD-B3LYP) with the 6-311 + G(2df) basis set at the optimized B3LYP/6-311 + G* geometry. In this approach, the first VDE was calculated at the B3LYP level as the lowest transition from the singlet state of the singly charged anion (B_{19}^-) into the final lowest doublet state of the neutral species (B_{19}) at the optimized geometry of the singly charged anion (B_{19}^-). Then the vertical excitation energies in the corresponding neutral species (at the TD-B3LYP level) were added to the lowest VDE to obtain the second and higher VDEs. All calculations were performed using the Gaussian 03 software package³⁶. Molecular orbital visualization was achieved using the Molekel 4.3 program³⁷.

Received 20 August 2009; accepted 10 December 2009;
published online 24 January 2010

References

- Minkin, V. I., Glukhovtsev, M. N. & Simkin, B. Y. *Aromaticity and Antiaromaticity* (Wiley, 1994).
- Schleyer, P. v. R. (ed.) Special edition on delocalization pi and sigma. *Chem. Rev.* **105** (2005).
- Schleyer, P. v. R. (ed.) Special edition on aromaticity. *Chem. Rev.* **101** (2001).
- Masamune, S., Hojo, K., Hojo Kiyomi, Bigam, G. & Rabenstein, D. L. Geometry of [10]annulenes. *J. Am. Chem. Soc.* **93**, 4966-4968 (1971).
- Masamune, S. & Darby, N. [10]Annulenes and other (CH)₁₀ hydrocarbons. *Acc. Chem. Res.* **5**, 272-281 (1972).
- King, R. A., Crawford, T. D., Stanton, J. F. & Schaefer, H. F. III. Conformations of [10]annulene: more bad news for density functional theory and second-order perturbation theory. *J. Am. Chem. Soc.* **121**, 10788-10793 (1999).
- Price, D. R. & Stanton, J. F. Computational study of [10]annulene NMR spectra. *Org. Lett.* **4**, 2809-2811 (2002).
- Li, X., Kuznetsov, A. E., Zhang, H. F., Boldyrev, A. I. & Wang, L. S. Observation of all-metal aromatic molecules. *Science* **291**, 859-861 (2001).
- Zhai, H. J., Alexandrova, A. N., Birch, K. A., Boldyrev, A. I. & Wang, L. S. Hepta- and octacoordinate boron in molecular wheels of eight- and nine-atom boron clusters: observation and confirmation. *Angew. Chem. Int. Ed.* **42**, 6004-6008 (2003).
- Zhai, H. J., Kiran, B., Li, J. & Wang, L. S. Hydrocarbon analogues of boron clusters - planarity, aromaticity and antiaromaticity. *Nature Mater.* **2**, 827-833 (2003).
- Alexandrova, A. N., Boldyrev, A. I., Zhai, H. J. & Wang, L. S. All-boron aromatic clusters as potential new inorganic ligands and building blocks in chemistry. *Coord. Chem. Rev.* **250**, 2811-2866 (2006).
- Zubarev, D. Yu. & Boldyrev, A. I. Comprehensive analysis of chemical bonding in boron clusters. *J. Comput. Chem.* **28**, 251-268 (2007).
- Fowler, J. E. & Ugalde, J. M. The curiously stable B_{13}^+ cluster and its neutral and anionic counterparts: the advantages of planarity. *J. Phys. Chem. A* **104**, 397-403 (2000).
- Mercero, J. M. & Ugalde, J. M. Sandwich-like complexes based on 'all-metal' (Al_4^{2-}) aromatic compounds. *J. Am. Chem. Soc.* **126**, 3380-3381 (2004).
- Aihara, J. B_{13}^+ is highly aromatic. *J. Phys. Chem. A* **105**, 5486-5489 (2001).
- Fowler, P. W. & Gray, B. R. Induced currents and electron counting in aromatic boron wheels: B_8^{2-} and B_9^- . *Inorg. Chem.* **46**, 2892-2897 (2007).
- Hanley, L. & Anderson, S. L. Production and collision-induced dissociation of small boron cluster ions. *J. Phys. Chem.* **91**, 5161-5163 (1987).
- Hanley, L., Whitten, J. L. & Anderson, S. L. Collision-induced dissociation and *ab initio* studies of boron cluster ions: determination of structures and stabilities. *J. Phys. Chem.* **92**, 5803-5812 (1988).
- Hintz, P. A., Ruatta, S. A. & Anderson, S. L. Interaction of boron cluster ions with water: single collision dynamics and sequential etching. *J. Chem. Phys.* **92**, 292-303 (1990).

20. Hintz, P. A., Sowa, M. B., Ruatta, S. A. & Anderson, S. L. Reactions of boron cluster ions (B_n^+ , $n = 2-24$) with N_2O : NO versus NN bond activation as a function of size *J. Chem. Phys.* **94**, 6446–6458 (1991).
21. Sowa-Resat, M. B., Smolanoff, J., Lapiki, A. & Anderson, S. L. Interaction of small boron cluster ions with HF *J. Chem. Phys.* **106**, 9511–9522 (1997).
22. Zhai, H. J., Wang, L. S., Alexandrova, A. N. & Boldyrev, A. I. Electronic structure and chemical bonding of B_5^- and B_5 by photoelectron spectroscopy and *ab initio* calculations. *J. Chem. Phys.* **117**, 7917–7924 (2002).
23. Alexandrova, A. N. *et al.* Structure and bonding in B_6^- and B_6 : planarity and antiaromaticity. *J. Phys. Chem. A* **107**, 1359–1369 (2003).
24. Zhai, H. J., Wang, L. S., Alexandrova, A. N., Boldyrev, A. I. & Zakrzewski, V. G. Photoelectron spectroscopy and *ab initio* study of B_3^- and B_4^- anions and their neutrals. *J. Phys. Chem. A* **107**, 9319–9328 (2003).
25. Kiran, B. *et al.* Planar-to-tubular structural transition in boron clusters: B_{20} as the embryo of single-walled boron nanotubes. *Proc. Natl Acad. Sci. USA* **102**, 961–964 (2005).
26. Sergeeva, A. P., Zubarev, D. Yu., Zhai, H. J., Boldyrev, A. I. & Wang, L. S. A photoelectron spectroscopic and theoretical study of B_{16}^- and B_{16}^{2-} : an all-boron naphthalene. *J. Am. Chem. Soc.* **130**, 7244–7246 (2008).
27. Zubarev, D. Yu. & Boldyrev, A. I. Revealing intuitively assessable chemical bonding patterns in organic aromatic molecules via adaptive natural density partitioning. *J. Org. Chem.* **73**, 9251–9258 (2008).
28. Wang, L. S., Cheng, H. S. & Fan, J. Photoelectron spectroscopy of size-selected transition metal clusters: Fe_n^- , $n = 3-24$. *J. Chem. Phys.* **102**, 9480–9493 (1995).
29. Saunders, M. Stochastic search for isomers on a quantum mechanical surface. *J. Comput. Chem.* **25**, 621–626 (2004).
30. Wales, D. J. & Doye, J. P. K. Global optimization by basin-hopping and the lowest energy structures of Lennard–Jones clusters containing up to 110 atoms. *J. Phys. Chem. A* **101**, 5111–5116 (1997).
31. Fujimori, M. *et al.* Peculiar covalent bonds in α -rhombohedral boron. *Phys. Rev. Lett.* **82**, 4452–4455 (1999).
32. Oger, E. *et al.* Boron cluster cations: transition from planar to cylindrical structures. *Angew. Chem. Int. Ed.* **46**, 8503–8506 (2007).
33. Zubarev, D. Yu. & Boldyrev, A. I. Developing paradigms of chemical bonding: adaptive natural density partitioning. *Phys. Chem. Chem. Phys.* **10**, 5207–5217 (2008).
34. Schleyer, P. v. R., Maerker, C., Dransfeld, A., Jiao, H. J. & Hommes, N. J. R. V. Nucleus-independent chemical shifts: a simple and efficient aromaticity probe. *J. Am. Chem. Soc.* **118**, 6317–6318 (1996).
35. Clar, E. *The Aromatic Sextet* (Wiley, 1972).
36. Frisch, M. J. *et al.* The Gaussian 03 program (revision D.01) (Gaussian, 2003).
37. Portmann, S. Molekel, Version 4.3 (Swiss National Supercomputing Centre/Swiss Federal Institute of Technology Zurich, 2002).

Acknowledgements

The experimental work was supported by the National Science Foundation (DMR-0904034). The basin-hopping search was performed with supercomputers at the EMSL Molecular Science Computing Facility, Pacific Northwest National Laboratory. The theoretical work done at Logan was supported by the National Science Foundation (CHE-0714851).

Author contributions

H.J.Z. performed the experiment. W.H. carried out the basin-hopping global minimum search. B.B.A. performed the Coalescence Kick global minimum search. A.P.S. carried out the geometry optimization and frequency calculations of all the B_{19}^- isomers recovered by the basin-hopping and the Coalescence Kick global minimum searches, and the calculations of VDEs, molecular orbital chemical bonding analyses and the AdNDP chemical bonding analyses. The experiment was designed by L.S.W. The data analyses were done by A.P.S., W.H., L.S.W. and A.I.B. The manuscript was written by A.P.S., L.S.W. and A.I.B., and was commented on by all the authors. A.I.B. and L.S.W. contributed equally to the study.

Additional information

The authors declare no competing financial interests. Supplementary information accompanies this paper at www.nature.com/naturechemistry. Reprints and permission information is available online at <http://npg.nature.com/reprintsandpermissions/>. Correspondence and requests for materials should be addressed to L.S.W. and A.I.B.